

**Arene-ligated Heteroleptic Terphenolate Complexes of Thorium**

Journal:	<i>Dalton Transactions</i>
Manuscript ID:	DT-ART-09-2014-002995.R1
Article Type:	Paper
Date Submitted by the Author:	09-Oct-2014
Complete List of Authors:	Arnold, Polly; University of Edinburgh, EaStCHEM School of Chemistry McKinven, Jamie; University of Edinburgh, EaStCHEM School of Chemistry Nichol, Gary; University of Edinburgh, Department of Chemistry; University of Edinburgh, EaStCHEM School of Chemistry

ARTICLE

Arene-ligated Heteroleptic Terphenolate Complexes of Thorium

Cite this: DOI: 10.1039/x0xx00000x

Jamie McKinven,^a Gary S. Nichol,^a and Polly L. Arnold^{a*}Received 00th January 2014,
Accepted 00th January 2014

DOI: 10.1039/x0xx00000x

www.rsc.org/

Bulky terphenolate ligands allow the synthesis of rare heteroleptic thorium chloride, and borohydride complexes; in the absence of donor solvents, the terphenolate ligands protect the metal ions through neutral Th- η^6 -arene interactions in a thorium bis (arene) sandwich motif.

Introduction

Homoleptic aryloxy complexes of the actinides have good literature precedent,¹⁻⁴ and have facilitated recent advances in actinide-mediated catalysis and the isolation of actinide compounds in which the metal has a rare assigned oxidation state.⁵⁻⁷ However, studies on the synthesis and reactivity of heteroleptic aryloxy complexes of actinides are scant, primarily due to difficulties associated with the ready ligand redistribution processes available to these large metal cations. Terphenolates were developed as particularly bulky ligands over a decade ago^{8,9} to support unusual chemistries and formal oxidation states in d- and p-block elements,¹⁰⁻¹³ whilst the terphenyl substituent has been incorporated as ligand substituents to enhance reactivity, for example enabling the catalytic conversion of dinitrogen to ammonia by molybdenum imido-alkylidene derivatives of the form [Mo(NR)(CHR')(OAr)(Pyr)] (where OAr is a terphenolate and Pyr is a pyrrolide).^{14,15} There are a few examples of their use with actinides: Heteroleptic uranyl [UO₂(O-2,6-Ph₂C₆H₃)₂(THF)₂] or uranium(IV) iodides [UI₃(O-2,6-Ph₂C₆H₃)(THF)₂] have been reported,^{16,17} but only a homoleptic, unsubstituted tetrakis(terphenolate) Th^{IV} complex [Th(O-2,6-Ph₂C₆H₃)₄] is known.¹⁸ The latter was reported to react with potassium metal to yield ligand-metallation products.¹⁸ We were interested in the potential for terphenolate

ligands to sterically protect a reaction space at a Th^{IV} centre in which the reactivity of small substrates could be explored. Herein, we describe the first synthesis and characterisation of heteroleptic substituted terphenolate complexes of thorium, and the ability of the ligand *ortho*-aryl substituents to provide a flexible, additional protection to the Th^{IV} cation.

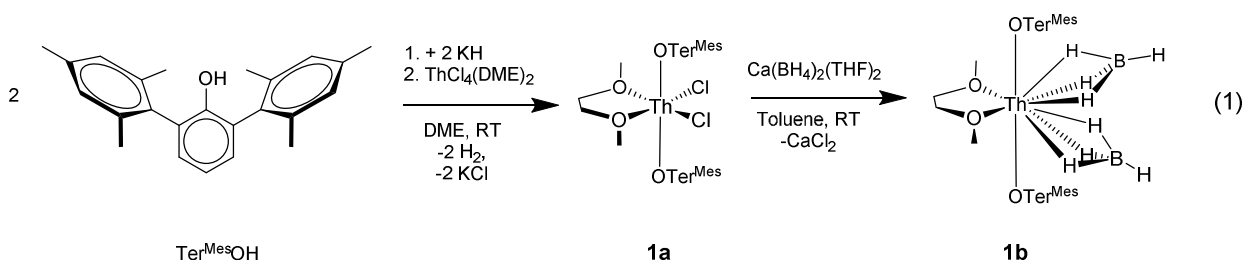
Results and Discussion

Synthesis of [Th(OTer^{Mes})₂Cl₂(DME)], **1a**

The reaction of ThCl₄DME₂ and two equivalents of KOTer^{Mes}, generated *in situ* by reaction of HOTer^{Mes} (C₂₄H₂₅OH) with KH, affords [Th(OTer^{Mes})₂Cl₂(DME)], **1a**, as an off-white solid in 66 % yield after workup (Equation 1). Single crystals suitable for X-ray diffraction of **1** were grown from a saturated solution of toluene at -30°C; the solid state structure is shown in **Figure 1a**.

Synthesis of [Th(OTerMes)₂(η^3 -BH₄)₂(DME)], **1b**

A salt elimination reaction between **1a** and Ca(BH₄)₂(THF)₂ in toluene generates [Th(OTerMes)₂(H₃BH)₂(DME)], **1b** as colourless crystals in 63 % yield after workup (Equation 1). The use of Ca(BH₄)₂(THF)₂ as a metathesis precursor for forming thorium borohydride complexes has precedent.¹⁹



Characterisation of **1a** and **1b**

Heteroleptic thorium borohydride complexes are rare, with only two other crystallographically characterised examples, $[\text{Th}(\text{N}(\text{SiMe}_3)_2)_3(\eta^3\text{-BH}_4)]$ and $[\text{Th}(\text{Ind}^*)_2(\eta^3\text{-BH}_4)_2]$ (Ind^* = permethylated indenyl) previously reported.^{19, 20} The BH_4 groups are readily identified in the NMR spectra as a broad shoulder under one of the DME proton resonances at 3.03 ppm in the ^1H NMR spectrum, and a poorly resolved pentet at -12.4 ppm in the ^{11}B NMR spectrum, which is resolved as a singlet upon proton decoupling. This is consistent with an averaged BH_4 proton environment on the NMR time scale. No boron NMR spectroscopic data were reported for other heteroleptic thorium borohydrides; for comparison the homoleptic $[\text{Th}(\text{H}_3\text{BCH}_3)_4]$ has a ^{11}B NMR spectral chemical shift at -19.3 ppm (also a quartet).²¹ The FTIR spectrum of **1b** displays weak absorptions consistent with $\eta^3\text{-BH}_4$ binding:²² $\nu(\text{B-H}_\mu)$ 2473 and 2455 cm^{-1} and $\nu(\text{B-H}_\parallel)$ 2225 and 2164 cm^{-1} . Single crystals suitable for x-ray diffraction of **1b** were grown from a saturated solution in toluene at -30°C .

Compound **1a** displays pseudo-octahedral geometry around the thorium cation, with two *trans*-oriented $\text{Ter}^{\text{Mes}}\text{O}^-$ ligands and a nearly linear O1-Th1-O2 bond angle ($179.1(2)^\circ$). This is atypical, and presumably a result of the steric bulk of the aryloxides as it is the most linear O-Th-O observed in six coordinate thorium aryloxide complexes.²³ The Th-O1,2 bonds are 2.180(3) Å, amongst the shortest reported Th-O single bonds, although they are significantly longer than the Th=O bond length of the thorium oxo-complex of 1.929(4) Å (molecular single Th-O bonds in the CSD range from 1.929 to 3.051 Å).^{23, 24} The solid-state molecular structure of **1b**, Figure 1b, is essentially the same as that of **1a**, although the O1-Th1-O2 angle of $158.5(2)^\circ$ is now significantly more bent than in **1a**. There is a notable difference between the Cl1-Th1-Cl1 angle in **1a**, $127.28(7)^\circ$, and the B1-Th1-B2 bond angle in **1b**, $96.00(2)^\circ$, presumably due the greater steric demand of the tridentate borohydride ligand and perhaps due to the greater π -bonding character of BH_4^- ligand compared to the Cl^- ligand, and its capacity for different bonding modes.²⁵ The Th-O1 bond distance of 2.191(4) Å in **1b**, is identical within s.u.s to the analogous bond distance in **1** of 2.180(3) Å.

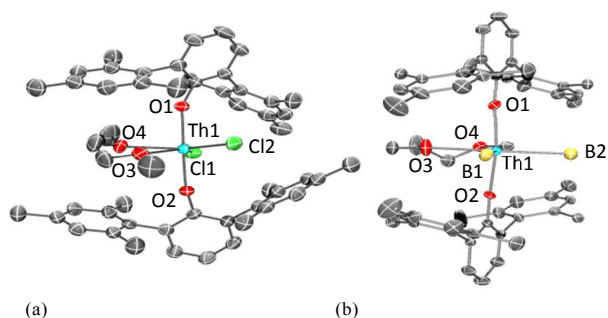
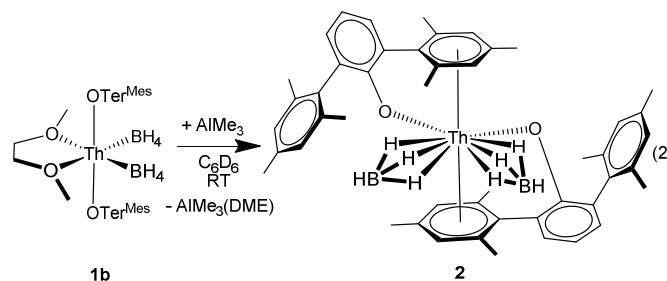


Figure 1: Displacement ellipsoid drawing of the solid-state molecular structure of **1a** (left) and **1b** (right) (50 % probability ellipsoids). Hydrogen atoms, solvent molecules and disorder in DME molecule are omitted for clarity.

A variety of experiments were undertaken with the target of removing the coordinated DME solvent from **1**. The application of dynamic vacuum (10^{-3} mbar over 12 hours) or heating in non-coordinating solvents (benzene, toluene, hexane) had no effect.

Synthesis of $\text{Th}(\text{OTer}^{\text{Mes}})_2(\eta^3\text{-BH}_4)_2$, **2**

The treatment of **1a** with trimethyl aluminium in toluene also yielded no reaction, but in the case of **1b** resulted in the abstraction of DME to afford $\text{AlMe}_3\cdot\text{DME}$ and the unusually low-coordinate $\text{Th}(\text{OTer}^{\text{Mes}})_2(\text{H}_3\text{BH}_4)_2$, **2**, as colourless needles in a 50 % yield after workup (Equation 2). We attribute this surprising contrast in reactivity to a very similar Lewis acidity of the two metal cations which are competing for the DME molecule. The $[\text{Th}^{\text{IV}}\text{Cl}_2]$ is a slightly harder, more strongly Lewis acid unit than the $[\text{Th}^{\text{IV}}(\text{BH}_4)_2]$ fragment, enabling the Al^{III} centre to out-compete the Th^{IV} centre for the O donor solvent in just the latter case.



Characterisation of **2**

Single crystals suitable for X-ray diffraction were grown by allowing a C_6D_6 solution of **2** to evaporate to dryness. The solid-state structure is displayed in Figure 2; one mesityl ring of each terphenolate ligand now participates in an η^6 -interaction with the thorium ion. The Th^{IV} cation is pseudo-octahedral, with the two η^6 -aryl interactions mutually *trans*, forming a weakly sandwiched thorium bis(arene) fragment. The Th^{IV} -arene centroid angle, Ct-Th-Ct, is close to linear, at 172.88° . The distance to one of the arenes is very long, and presumably a very weak interaction, characterised by a Th-Ct1 distance of 4.05(1) Å, whilst the other is short, with a Th-Ct2 distance of 2.815(3) Å, although still relatively long compared with the few other examples of $\text{Th}-\eta^6$ -arene interactions (A survey of the CSD found that neutral η^6 -Th-Ct distances in the literature range from 2.706 to 2.950 Å).^{23, 26-28} These Th-Ct distances are longer than the macrocyclic neutral phenyl interactions observed in $[\text{ThCl}_3(\kappa^2\text{-NC}_4\text{H}_4\text{C}[\text{CH}_3]_2)_2(\eta^6\text{-C}_6\text{H}_4)(\text{Li}[\text{DME}]_3)]$ and $[\text{ThCl}_2(\kappa^2\text{-NC}_4\text{H}_4\text{C}[\text{CH}_3]_2)(\eta^6\text{-C}_6\text{H}_4)(\mu^2\text{PhNNPh})(\text{Li}[\text{DME}])]$ by Gambarotta *et al.* The mesityl rings that participate in η^6 -aryl interactions deviate from the parallel by 24.49° . The two O atoms and two B atoms are approximately coplanar, with a deviation of O1TerMes- (that which displays the weaker Th-arene interaction) of 28.54° out of the plane. The TerMesO- ligands are *cis*-disposed as evidenced by the O1-Th1-O2 bond angle of $89.0(3)^\circ$, substantially smaller than the corresponding angle in **1b**. The

B1-Th1-B2 bond angle of **2**, $92.9(7)^\circ$, represents a contraction of this angle compared to **1b**.

The room-temperature ^1H NMR spectrum of a benzene solution of **2** contains a single environment for the $\text{Ter}^{\text{Mes}}\text{O}^-$ protons, suggesting a dynamic equilibrium is present on the NMR timescale that interconverts the free and Th-bound Mes groups. Similarly to **2**, the $[\text{BH}_4]^-$ groups appear as a broad resonance at -0.39 ppm in the ^1H NMR spectrum and as a poorly resolved pentet at -10.08 ppm in the ^{11}B NMR spectrum which resolves into a singlet upon proton decoupling. However, the FTIR spectrum of **2** displays weak absorptions characteristic of an $\eta^3\text{-BH}_4$ binding mode ($2500\text{--}2200\text{ cm}^{-1}$).²² $\nu(\text{B-H}_i)$ 2474 cm^{-1} and $\nu(\text{B-H}_u)$ 2216 and 2149 cm^{-1} . Hydrogen atoms were not located in the solid-state structure of **2** (Figure 2) but the Th-B distance has increased from $2.640(1)\text{ \AA}$ in **1b** to $2.670(2)\text{ \AA}$.

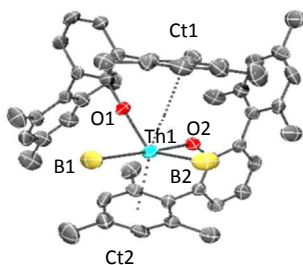
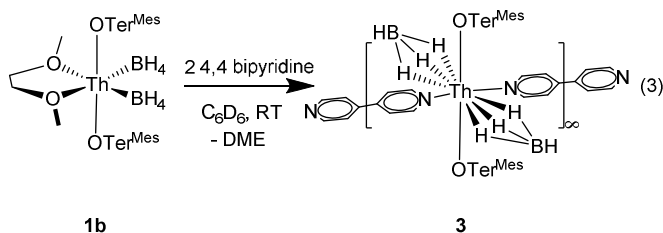


Figure 2: Displacement ellipsoid drawing of the solid-state molecular structure of **2** (50 % probability ellipsoids). Hydrogen atoms are omitted for clarity.

Synthesis of $[\text{Th}(\text{OTer}^{\text{Mes}})_2(\eta^3\text{-BH}_4)_2(4,4\text{-NC}_5\text{H}_4\text{C}_5\text{H}_4\text{N})]_\infty$, **3**

Treatment of **1a** with two equivalents of 4,4-bipyridine successfully displaces the coordinated DME to afford a coordination polymer $[\text{Th}(\text{OTer}^{\text{Mes}})_2(\text{H}_3\text{BH})_2(4,4\text{-NC}_5\text{H}_4\text{C}_5\text{H}_4\text{N})]_\infty$, **3**, which crystallises readily and cleanly out of the reaction mixture as yellow crystals, equation 3. The solid state structure of a single repeat unit of **3** is displayed in Figure 3.



Characterisation of **3**

In **3** the *pseudo*-octahedral Th^{IV} centre still has two *trans*-disposed OTer^{Mes} ligands with the same angle ($179.00(6)^\circ$) as in **1a** (within s.u.s). In contrast, the two BH_4 ligands are also now mutually *trans*, as evidenced by a B1-Th1-B1 angle of $167.33(10)^\circ$, allowing the *trans*-4,4-bipyridine ligation to generate nearly linear 1-D polymeric chains (see Figure 5) in the solid state; the complex crystallises directly from the reaction mixture. The Th1-Th1-Th1 angle of $152.40(5)^\circ$ shows that there is a significant undulation in the polymeric chain. The

two OTer^{Mes} central aryloxy C_6 planes are now orthogonal, whereas in **1a**, **1b** and **2** they are parallel, presumably due to avoid interactions with the coordinated bipyridine. The Th-O bonds are both short, $2.168(2)$ and $2.210(2)\text{ \AA}$, with Th-O1 being shorter, perhaps due to a π -stacking between one of the mesityl rings on $\text{O1Ter}^{\text{Mes}}$ and the 4,4-bipyridyl ligand (Ct1-Ct2 distance $3.74(7)\text{ \AA}$). Both Th-O bond lengths, as for **1a**, **1b** and **2** remain short for Th-O bonds. The Th-N bond distances in **3**, of $2.626(2)$ and $2.644(2)\text{ \AA}$, are typical. The $[\text{BH}_4]^-$ group is observed as a broad resonance at 3.28 ppm in the ^1H NMR spectrum and as a broad singlet at -6.42 ppm in the ^{11}B NMR spectrum, which sharpens upon proton decoupling, consistent with an averaged BH_4^- proton environment on the NMR timescale. The FTIR spectrum of **3** contains weak absorptions in the $2500\text{--}2200\text{ cm}^{-1}$ region consistent with a $(\mu\text{-H})_3$ binding mode.²² $\nu(\text{B-H}_i)$ 2454 cm^{-1} and $\nu(\text{B-H}_u)$ 2237 and 2171 cm^{-1} . The Th-B bond lengths in **3**, of $2.666(3)$ and $2.673(3)\text{ \AA}$, are comparable to those seen in **2** and slightly longer than those in **1b**.

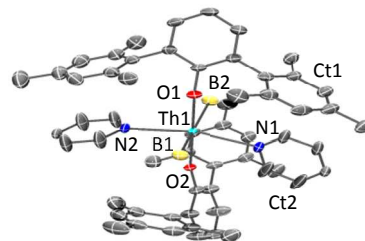
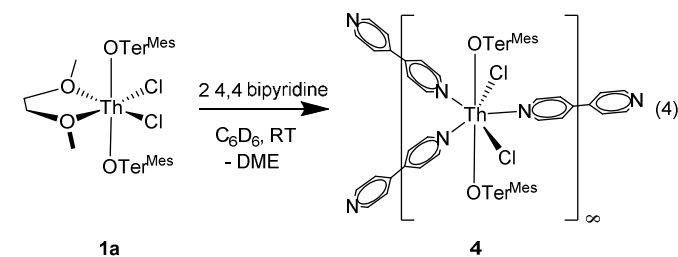


Figure 3: Displacement ellipsoid drawing of the solid-state molecular structure of the monomeric unit of **3** (50 % probability ellipsoids). Hydrogen atoms and toluene solvent molecules are omitted for clarity.

Synthesis of $[\text{Th}(\text{OTer}^{\text{Mes}})_2(\text{Cl})_2(4,4\text{-bipyridyl})_{1.5}]_\infty$, **4**

Treatment of **1b** with two equivalents of 4,4 bipyridine successfully displaces the coordinated DME to afford a coordination polymer $[\text{Th}(\text{OTer}^{\text{Mes}})_2(\text{Cl})_2(4,4\text{-bipyridyl})_{1.5}]_\infty$, **4**, which crystallises readily and easily out of the reaction mixture as colourless needles, Equation 4. The solid state structure of a single repeat unit of **4** is displayed in Figure 4.



Characterisation of **4**

In **4** the Th^{IV} centre has adopted a *pseudo*-pentagonal bipyramidal structure with 3 N-donor bipyridyl ligands and two chloride ligands in the equatorial plane whilst retaining the two *trans* disposed OTer^{Mes} ligands at $177.78(11)^\circ$. In **4** the Cl-Th-Cl angle of $159.24(4)^\circ$ is wider when compared to **1a**, presumably to enable the ligation of three donor ligands in the

equatorial plane. The equatorial ligands show significant deviations from the plane as evidenced by the angles O_1-Th_1-X (where X is the bonding atom in the plane.) The O_1-Th_1-Cl angles of $94.96(10)$ and $86.44(10)^\circ$ are close to perpendicular but the O_1-Th_1-N angles of $103.94(12)$, $78.34(12)$ and $88.20(15)^\circ$ indicate a substantial deviation from the plane. The increased number of donor ligands compared to **3**. The increased number of donor ligands also results in three $Th_1-Th_1-Th_1$ angles of $144.97(9)$, $150.32(9)$ and $64.66(9)^\circ$. The first two of these angles are comparable to the analogous angle observed in **3**, whilst the third generates zig-zag shaped $Th(bipy)Th(bipy)Th$ chains that build the overall 2-D polymer (Figure 6).

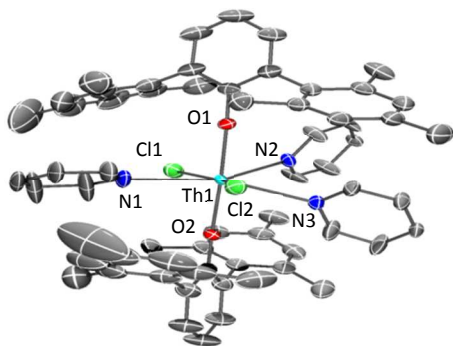


Figure 4: Displacement ellipsoid drawing of the solid-state molecular structure of the monomeric unit of **4** (50 % probability ellipsoids). Hydrogen atoms and lattice benzene and bipyridine molecules removed for clarity.

The two $OTer^{Mes}$ central aryl groups are, as seen in **3** orthogonal to each other; this is again likely to minimise the interactions with the bipyridine ligands. The Th-O bonds, $2.221(3)$ and $2.232(3)$ Å, are longer than those seen in **1-3**, but remain short for Th-O bonds. This slight lengthening is to be expected from the increased electron donation that a third N-donor ligand provides, increasing the electron density on thorium, and thus reducing the electrostatic interaction with the $OTer^{Mes}$ ligand. The Th-N bond distances in **4**, of $2.695(4)$, $2.667(5)$ and $2.677(4)$ Å are typical. The Th-Cl bond distances in **4**, of $2.698(2)$, $2.710(2)$ Å, are also typical.

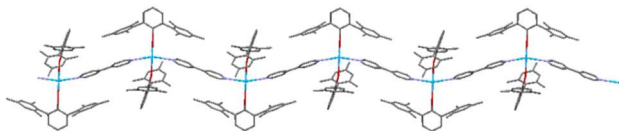


Figure 5: A portion of the 1-D polymeric chain structure of **3**. Hydrogen atoms and toluene solvent molecules removed for clarity.

As a donor, 4,4-bipyridine has been used extensively to bridge two metal centres to form co-ordination polymers, particularly for transition metals.²⁹ There are few known actinide compounds containing 4,4-bipyridine as a bridging ligand and all involve uranium.³⁰ The U-N bond distances are very similar to the Th-N distance in **3**. To the best of our knowledge, **3** and **4** are the first compounds in which two thorium centres are

bridged by 4,4-bipyridine, and only the second example of 4,4-bipyridine acting as a ligand towards thorium.³¹ Complexes **3** and **4** have shorter Th-N bond distances than the first reported example, $[Th(\eta-C_8H_8)_2(4,4-bipyridyl)](2.707(2)$ Å).³¹ The well-documented ability of bipyridyls to accept electrons may provide a route to reduced analogues of **3** or **4**.

The main distinction between the polymeric structures of **3** and **4** lies in the type of polymer produced; **3** is a 1-D polymeric chain, whilst **4** forms 2-d polymeric sheets. This is a direct consequence of the number of bipyridine molecules that are ligated to the thorium centre, i.e. two *trans*-oriented molecules in **3** leads to a chain structure, whilst three molecules in a pentagonal equatorial plane leads to a 2D sheet structure. A further difference is that **4** contains voids of radius 1.2 Å (similar to the size of dihydrogen gas) which makes up 6.3% of the unit cell volume, whilst **3** does not contain any voids of this size.

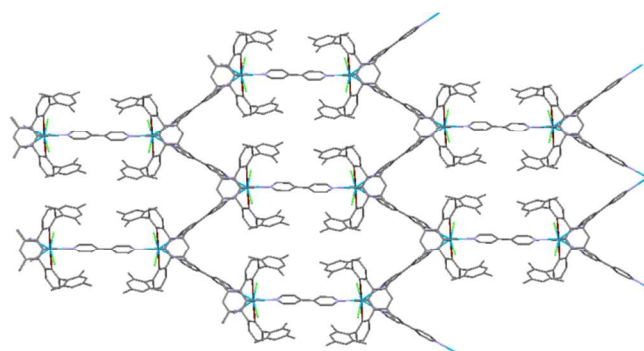


Figure 6: A portion of the 2-D polymeric chain structure of **4**. Hydrogen atoms and lattice benzene and bipyridine molecules removed for clarity.

Of note here is that **3** is soluble in benzene and non-coordinating solvents. This is not normally the case for coordination polymers which need, at the minimum, a suitable additional donor to terminate the oligomer ends or fully break up the polymer. We suggest that the demonstrated ability of the terphenolate arene groups to bind to the metal centres may allow **2** to form monomers in non-polar solvents, allowing for the ready dissolution of the polymeric structure.

Experimental

General Methods

All manipulations were carried out using standard Schlenk line or glovebox techniques under an atmosphere of dinitrogen unless otherwise stated. DME was distilled from sodium under dinitrogen in a solvent still prior to use. Hexane, diethyl ether and toluene were degassed by sparging with dinitrogen and dried by passing through a column of activated sieves in Vacuum Atmospheres solvent towers. Solvents were stored over activated 4 Å molecular sieves. Deuterated solvents (d_8 -toluene and C_6D_6) were boiled over potassium, vacuum-transferred and freeze-pump-thaw degassed three times prior to use.

^1H NMR and $^{13}\text{C}\{^1\text{H}\}$ NMR spectra were recorded on a Bruker PRO500 spectrometer operating at 499.90 and 125.76 MHz respectively. ^{11}B and $^{11}\text{B}\{^1\text{H}\}$ NMR spectra were recorded at 298 K on a Bruker PRO500 at 160.49 MHz and were referenced to external $\text{BF}_3\cdot\text{OEt}_2$. Chemical shifts are reported in parts per million and referenced to residual proton resonances calibrated against external TMS ($\delta = 0$ ppm). All spectra were recorded at 298 K unless otherwise stated.

Elemental analyses were carried out by Mr. Stephen Boyer, London Metropolitan University, Analytische Laboratorien Germany and Medac Ltd UK. Infrared spectra were recorded on a Jasco 410 spectrophotometer, w = weak, m = medium, s = strong intensity on in a Nujol mull on BaF_2 or NaCl plates. BaF_2 plates do not allow transmission below 1000 cm^{-1} .

$\text{HOTer}^{\text{Mes}}$ was synthesised according to literature procedures.^{8, 9, 32, 33} $\text{Ca}(\text{BH}_4)_2\cdot\text{THF}_2$ was purchased from Sigma Aldrich and used as received.

Synthetic Procedures

1a [$\text{Th}(\text{OTer}^{\text{Mes}})_2\text{Cl}_2(\text{DME})$]

To a Schlenk charged with a stirrer bar and $\text{HOTer}^{\text{Mes}}$ (1.3955g, 4.22 mmol), was added *circa* 40 ml of dry DME, forming a brown solution. This solution was cannulated onto KH (169.3 mg, 4.22 mmol), causing vigorous effervescence and the formation of a light brown suspension which was allowed to stir for 2 hours. This suspension was then cannulated onto a DME suspension of $\text{ThCl}_4(\text{DME})_2$ causing the formation of a dark brown suspension which was allowed to stir overnight. The suspension was filtered to separate a red-brown solution from a grey powder. Volatiles were removed from the filtrate *in vacuo* and the resultant brown residue was extracted with toluene, and then concentrated and cooled to -30°C , which caused the formation of colourless crystals of **1a**, (1.4683g, 1.39 mmol, 66% yield). Single crystals suitable for X-ray crystallography were grown from a saturated solution of toluene held at a temperature of -30°C . Elemental analysis; calculated: C 61.23%, H 5.93%; found: C 61.38%, H 6.04%. ^1H NMR (500 MHz) δ 6.97 (t, $J = 1.7$ Hz, 1H, para C-H), 6.93 (d, $J = 1.7$ Hz, 2H, meta C-H), 6.87 (s, 4H, mesityl aromatic C-H), 3.15 (s, 3H, $\text{CH}_3\text{OCH}_2\text{CH}_2\text{OCH}_3$), 2.27 (s, 12H, Ortho CH_3), 2.26 (s, 6H, Para CH_3), 2.02 (s, 2H, $\text{CH}_3\text{OCH}_2\text{CH}_2\text{OCH}_3$). $^{13}\text{C}\{^1\text{H}\}$ NMR (500 MHz) δ (ppm) 161.42 (q, C1), 137.36 (q, C2, C6), 135.84 (q, C7, C16), 131.60 (q, C8, C12, C17, C21), 129.96 (s, C4), 129.33 (q, C10, C19), 128.71 (s, C9, C11, C18, C20), 120.49 (s, C3, C5), 72.22 (s, $\text{CH}_3\text{OCH}_2\text{CH}_2\text{OCH}_3$ [C26,C27]), 63.49 (s, $\text{CH}_3\text{OCH}_2\text{CH}_2\text{OCH}_3$ [C25,C29]), 21.54 (s, C13, C15, C22, C24), 21.30 (s, C14, C23).

1b [$\text{Th}(\text{OTer}^{\text{Mes}})_2(\eta^3\text{-BH}_4)_2(\text{DME})$]

To a Schlenk charged with a stirrer bar and **1a** (150 mg, 0.142 mmol), was added *circa* 20 ml of dry toluene, forming an orange- brown solution. To this solution was added a colourless solution of $\text{Ca}(\text{BH}_4)_2\cdot\text{THF}_2$ (30.5 mg, 0.142 mmol) in toluene forming a pale yellow suspension upon addition. After 2 days of stirring, this suspension had become colourless. The

suspension was filtered to give a colourless solution, and this solution was concentrated and cooled to -30°C , to give colourless crystals of **1b**, (87.3 mg, 0.089 mmol, 63% yield). Single crystals suitable for X-ray crystallography were grown from a saturated solution of toluene held at a temperature of -30°C . Elemental analysis; calculated: C 61.79%, H 6.78%, found: C 61.64%, H 6.82%. ^1H NMR (500 MHz, C_6D_6) δ 6.88 (s, 2H), 6.85 (s, 1H), (overlapping aromatic para and ortho protons of central phenyl ring), 6.81 (s, 4H) (meta C-H), 3.03 (s, 7H) (overlapping BH_4 and $\text{CH}_3\text{OCH}_2\text{CH}_2\text{OCH}_3$), 2.25 (s, 6H) (para CH_3), 2.18 (s, 12H) (ortho CH_3), 2.12 (s, 2H) ($\text{CH}_3\text{OCH}_2\text{CH}_2\text{OCH}_3$). ^{11}B NMR (160 MHz, C_6D_6) δ -12.46 (p). $^{11}\text{B}\{^1\text{H}\}$ NMR (160 MHz, C_6D_6) δ -12.42 (s). ^{13}C NMR (126 MHz, C_6D_6) δ 161.76 (s), 138.27 (s), 137.19 (s), 135.95 (s), 131.52 (s), 130.44 (s), 129.95 (s), 129.34 (s), 128.88 (s), 128.69 (s), 128.57 (s), 128.35 (s), 125.70 (s), 120.08 (s), 72.64 (s), 64.38 (s), 21.67 (s), 21.22 (s). FTIR Spectroscopy (Nujol mull on BaF_2 Plates) 2726 (m), 2474 (m), 2456 (m), 2226 (m), 2164 (m), 1460 (s), 1377 (s) cm^{-1} .

2 $\text{Th}(\text{OTer}^{\text{Mes}})_2(\eta^3\text{-BH}_4)_2$

To a Schlenk charged with a stirrer bar and **1b** (208.1 mg, 0.206 mmol), was added *circa* 20 ml of dry toluene, forming a yellow-orange solution. To this solution was added *via* syringe a solution of AlMe_3 in hexanes (2.0M, 0.21ml, 0.41 mmol), causing a lightening of the solution to yellow, and subsequent formation of a fine suspension. After stirring overnight, the suspension was filtered to yield a pale yellow solution. This solution was concentrated and cooled to -30°C , to give white needles of **2**, (95.3 mg, 0.104 mmol, 50% yield). Single crystals suitable for X-ray crystallography were grown from a saturated solution of toluene stored at -30°C . Elemental analysis; calculated: C 62.62%, H 6.36%, found: C 62.48%, H 6.44%. ^1H NMR (500 MHz, C_6D_6) δ 6.88 (d, $J = 2.9$ Hz, 1H), 6.87 (s, 2H), 6.79 (s, 4H), 3.12 (s, 11H), 2.83 (s, 14H), 2.24 (s, 6H), 2.08 (s, 12H), -0.39 (s, 4H) (BH_4). ^{13}C NMR (126 MHz, C_6D_6) δ 161.38 (s), 148.00 (s), 141.99 (s), 139.50 (s), 139.26 (s), 138.61 (s), 138.46 (s), 137.47 (s), 137.21 (s), 136.46 (s), 135.79 (s), 135.39 (s), 130.77 (s), 130.46 (s), 130.24 (s), 130.16 (s), 130.06 (s), 129.37 (s), 128.99 (s), 128.87 (s), 128.68 (s), 128.51 (s), 128.35 (s), 128.16 (s), 127.97 (s), 127.74 (s), 120.72 (s), 120.05 (s), 21.66 (s), 21.48 (s), 21.28 (s), 21.25 (s), 21.16 (s), 20.98 (s), 20.84 (s), 20.50 (s). ^{11}B NMR (160 MHz, C_6D_6) δ -10.08 (p). $^{11}\text{B}\{^1\text{H}\}$ NMR (160 MHz, C_6D_6) δ -10.08 (s). FTIR Spectroscopy (Nujol mull on NaCl plates) 2957 (s), 2922 (s), 2853 (s), 2474 (m), 2217 (m), 2149(m), 1611 (m), 1455 (m) cm^{-1} .

3 [$\text{Th}(\text{OTer}^{\text{Mes}})_2(\eta^3\text{-BH}_4)_2(4,4\text{-NC}_5\text{H}_4\text{C}_5\text{H}_4\text{N})$]

To a pale yellow solution of **1b** (10 mg, 0.010 mmol) in d_8 -toluene (0.6 mL) in a Teflon-valved valve NMR tube was added as a white crystalline solid 4,4 bipyridine (3 mg, 0.020 mmol, 2 equiv) resulting in a yellow solution. Transfer of the solution to a vial, and allowing this solution to stand resulted in the formation of yellow crystals of **3**, (7.0 mg, 0.006 mmol, 66% yield) suitable for single crystal X-ray crystallography.

Elemental analysis; calculated: C 64.69%, H 6.18%, N 2.60% found: C 64.44%, H 5.85%, N 2.72% ¹H NMR (500 MHz, C₇D₈) δ 7.01 (s, 2H), 6.97 (s, 4H), 6.81 (s, 1H), 6.74 (s, 4H), 6.55 (s, 4H), 3.28 (s, 4H) (BH₄), 2.08 (s, 6H), 2.00 (s, 12H). ¹³C NMR (126 MHz, C₆D₆) δ 161.69 (s), 150.69 (s), 145.30 (s), 137.18 (s), 135.79 (s), 129.33 (s), 120.94 (s), 119.97 (s), 21.72 (s), 20.54 (s). ¹¹B NMR (160 MHz, C₇D₈) δ -6.42 (s). FTIR Spectroscopy (Nujol mull on NaCl Plates) 2938 (s), 2901 (s), 2831 (s), 2454 (m), 2237 (m), 2171(m), 1618 (m), 1458 (m) cm⁻¹.

4 [Th(OTer^{Mes})₂(Cl)₂(4,4-bipyridyl)_{1.5}]

To a brown solution of **1a** (10 mg, 0.010 mmol) in C₆D₆ (0.6 mL) in a Teflon-valved valve NMR tube was added as a white crystalline solid 4,4 bipyridine (3 mg, 0.020 mmol, 2 equiv) resulting in a brown-orange solution. Allowing this solution to stand at room temperature resulted in the formation of colourless needles of **4**, (5.0 mg, 0.005 mmol, 47% yield) suitable for single crystal X-ray crystallography. ¹H NMR (500 MHz, C₆D₆) δ 7.01 (d, *J* = 1.6 Hz, 1H), 7.00 (s, 4H), 6.84 (s, 4H), 6.78 (s, 4H), 6.51 (s, 4H), 6.28 (d, *J* = 0.8 Hz, 2H), 2.19 (s, 12H), 2.15 (s, 6H), 2.11 (s, 12H), 2.07 (s, 6H).

Conclusions

To conclude, we have described the synthesis and characterisation of the first examples of heteroleptic terphenolate complexes of thorium. Complex **1a** is a good precursor for rare, crystallographically characterised examples of thorium borohydride complexes. In contrast to the dichloride complex **1a**, the borohydride ligands in **1b** render the Th^{IV} centre sufficiently 'soft' that the Lewis acidic centre Al^{III} is able to abstract the coordinated DME from only the latter, yielding complex **2** with two stabilising Th-η-arene interactions. The formation of reversible, neutral Th-η⁶-arene interactions crystallographically characterised in **2**, and suggested by the solubility of the rare one-dimensional co-ordination polymer **3**, confirms the suitability of TerMesO⁻ as a strongly binding σ-O-donor ancillary ligand for actinide cations with a flexible steric protection that can participate in π/δ-stabilising interactions.

Acknowledgements

The authors are grateful for the support of the Technische Universität München – Institute for Advanced Study, funded by the German Excellence Initiative, EaStCHEM, the University of Edinburgh, and the EPSRC.

Notes and references

^a EaStCHEM School of Chemistry, Joseph Black Building, University of Edinburgh, The Kings' Buildings, Edinburgh, EH9 3JJ, UK.

† Electronic Supplementary Information (ESI) available: Full synthetic and crystallographic details for the complexes. See DOI: 10.1039/c000000x/. CCDC codes for the structures are CCDC 1019326-1019329 and 1020471.

1. T. Andrea, E. Barnea, M. Botoshansky, M. Kapon, E. Genizi, Z. Goldschmidt and M. S. Eisen, *J. Organomet. Chem.*, 2007, **692**, 1074-1080.
2. L. Salmon, P. Thuéry, E. Rivière and M. Ephritikhine, *Inorg. Chem.*, 2005, **45**, 83-93.
3. J. M. Berg, D. L. Clark, J. C. Huffman, D. E. Morris, A. P. Sattelberger, W. E. Streib, W. G. Van der Sluys and J. G. Watkin, *J. Am. Chem. Soc.*, 1992, **114**, 10811-10821.
4. S. Fortier, G. Wu and T. W. Hayton, *Inorg. Chem.*, 2009, **48**, 3000-3011.
5. H. S. La Pierre, H. Kameo, D. P. Halter, F. W. Heinemann and K. Meyer, *Angew. Chem., Int. Ed. Engl.*, 2014, **53**, 7154-7157.
6. H. S. La Pierre, A. Scheurer, F. W. Heinemann, W. Hieringer and K. Meyer, *Angew. Chem., Int. Ed. Engl.*, 2014, **53**, 7158-7162.
7. S. M. Franke, B. L. Tran, F. W. Heinemann, W. Hieringer, D. J. Mindiola and K. Meyer, *Inorg. Chem.*, 2013, **52**, 10552-10558.
8. C. Stanciu, Marilyn M. Olmstead, Andrew D. Phillips, M. Stender and Philip P. Power, *Eur. J. Inorg. Chem.*, 2003, **2003**, 3495-3500.
9. D. A. Dickie, I. S. MacIntosh, D. D. Ino, Q. He, O. A. Labeodan, M. C. Jennings, G. Schatte, C. J. Walsby and J. A. C. Clyburne, *Can. J. Chem.*, 2008, **86**, 20-31.
10. C. Stanciu, A. F. Richards, M. Stender, M. M. Olmstead and P. P. Power, *Polyhedron*, 2006, **25**, 477-483.
11. B. D. Rekken, T. M. Brown, M. M. Olmstead, J. C. Fettinger and P. P. Power, *Inorg. Chem.*, 2013, **52**, 3054-3062.
12. C. S. Weinert, P. E. Fanwick and I. P. Rothwell, *Dalton Trans.*, 2003, 1795-1802.
13. M. Carrasco, R. Peloso, A. Rodriguez, E. Alvarez, C. Maya and E. Carmona, *Chem. - Eur. J.*, 2010, **16**, 9754-9757, S9754/9751-S9754/9769.
14. R. R. Schrock, A. J. Jiang, S. C. Marinescu, J. H. Simpson and P. Müller, *Organometallics*, 2010, **29**, 5241-5251.
15. E. M. Townsend, R. R. Schrock and A. H. Hoveyda, *J. Am. Chem. Soc.*, 2012, **134**, 11334-11337.
16. M. P. Wilkerson, C. J. Burns, D. E. Morris, R. T. Paine and B. L. Scott, *Inorg. Chem.*, 2002, **41**, 3110-3120.
17. D. D. Schnaars, G. Wu and T. W. Hayton, *Dalton Trans.*, 2009, 3681-3687.
18. I. Korobkov, A. Arunachalampillai and S. Gambarotta, *Organometallics*, 2004, **23**, 6248-6252.
19. T. M. Trnka, J. B. Bonanno, B. M. Bridgewater and G. Parkin, *Organometallics*, 2001, **20**, 3255-3264.
20. H. W. Turner, R. A. Andersen, A. Zalkin and D. H. Templeton, *Inorg. Chem.*, 1979, **18**, 1221-1224.
21. R. Shinomoto, J. G. Brennan, N. M. Edelstein and A. Zalkin, *Inorg. Chem.*, 1985, **24**, 2896-2900.
22. T. J. Marks and J. R. Kolb, *Chem. Rev.*, 1977, **77**, 263-293.
23. F. Allen, *Acta Crystallographica Section B*, 2002, **58**, 380-388.
24. W. Ren, G. Zi, D.-C. Fang and M. D. Walter, *J. Am. Chem. Soc.*, 2011, **133**, 13183-13196.
25. D. Hohl and N. Roesch, *Inorg. Chem.*, 1986, **25**, 2711-2718.
26. C. A. Cruz, D. J. H. Emslie, L. E. Harrington and J. F. Britten, *Organometallics*, 2007, **27**, 15-17.
27. I. Korobkov, B. Vidjayacoumar, S. I. Gorelsky, P. Billone and S. Gambarotta, *Organometallics*, 2010, **29**, 692-702.

Dalton Transactions

28. C. A. Cruz, D. J. H. Emslie, C. M. Robertson, L. E. Harrington, H. A. Jenkins and J. F. Britten, *Organometallics*, 2009, **28**, 1891-1899.
29. K. Biradha, M. Sarkar and L. Rajput, *Chem. Commun.*, 2006, 4169-4179.
30. T. Kawasaki, T. Nishimura and T. Kitazawa, *Bull. Chem. Soc. Jpn.*, 2010, **83**, 1528-1530.
31. J.-C. Berthet, P. Thuéry, N. Garin, J.-P. Dognon, T. Cantat and M. Ephritikhine, *J. Am. Chem. Soc.*, 2013, **135**, 10003-10006.
32. K. Ruhlandt-Senge, J. J. Ellison, R. J. Wehmschulte, F. Pauer and P. P. Power, *J. Am. Chem. Soc.*, 1993, **115**, 11353-11357.
33. B. Schiemenz and P. P. Power, *Organometallics*, 1996, **15**, 958-964.